# Behavior of a Magnetic Fluid Microdrop in a Rotating Magnetic Field

J.-C. Bacri,[1,*] A. Cebers,[2] and R. Perzynski[1]

[1]*Laboratoire d'Acoustique et Optique de la Matière Condensée, Université Pierre et Marie Curie, Tour 13, Boîte 78, 4 place Jussieu, 75252 Paris Cedex 05, France*

[2]*Institute of Physics, Latvian Academy of Sciences, LV-2169 Riga, Salaspils-1, Latvia*

(Received 16 September 1992)

The response of a magnetic fluid microdrop to a rotating magnetic field is studied for the first time. An unexpected shape instability is observed, leading to the formation of a spiny starfish shape that slowly corotates with the field. A simple model accounts for (i) the stability range of an oblate ellipsoidal shape that is a precursor to the starfish, (ii) the rotational frequency which is substantially lower than that of the applied magnetic field, and (iii) a lateral peak instability that is responsible for growth of the spiny arms of the starfish.

PACS numbers: 47.20.−k, 47.35.+i, 75.50.Mm

In the study of pattern formation, physicists are concerned with simple figures; a spherical liquid droplet is one of the simplest. In his pioneering works, applied to the mechanics of heavenly bodies and the shape of galaxies [1], Poincaré calculated equilibrium figures of a rotating fluid mass, taking into account gravitational and centrifugal energies, and neglecting surface energy. He predicted a series of shape instabilities between various ellipsoids (oblate, prolate, Jacobi,...) and even predicted the possibility of observing a torus (Saturn's ring). The tensor virial method [2] has been introduced by Chandrasekhar to study the stability of a rotating drop held together by surface tension.

On a laboratory scale, various experiments have been performed in the past on free liquid droplets distorted by an elongating static external field: for instance, a drop of dielectric liquid subjected to an electric field [3], a viscous drop in an elongational flow [4], and a magnetic fluid (MF) drop in a static magnetic field [5]. The transient problem of the spreading of a drop lying on a solid surface has also been investigated both experimentally and theoretically by Tanner [6], de Gennes [7], and Melo, Joanny, and Fauve [8]. The latter flows yield spreading instabilities and fingering, governed either by surface tension gradients [9,10] or centrifugal forces [8].

We report here on the first experiment dealing with a droplet submitted concomitantly to both a radial and a tangential stress. The system is a buoyant MF drop acted on by a rotating magnetic field. We observe, for the first time, a transition from an oblate shape to a prolate shape followed by transition back to another thin and flat oblate shape, similar to the predictions of Poincaré and Chandrasekhar. The well-known classical peak instability of MF, which in this case occurs all around the rotating oblate drop, crowns the drop with peaks making it look like a starfish.

The MF used in our study is ionic ferrofluid composed of a colloidal dispersion of monodomain magnetic particles, of typical size 10 nm, dispersed in an aqueous solution. The colloidal stability of an ionic ferrofluid is governed by screened electrostatic repulsion between grains [11]: A phase separation into two liquid phases can be induced by an increase of ionic strength leading to the formation of microdrops of a highly magnetic MF surrounded by the coexisting dilute phase. Microdrops have a typical radius of 10 $\mu$m in zero field and 25% volume of magnetic particles. Such magnetic droplets are easily deformable in weak uniform magnetic fields on the order of a few 100 A/m. They assume an elongated shape determined by a balance of magnetic forces which tend to elongate and surface tension forces which tend to restore sphericity. Measurements of static and dynamic elongations [5] are used to determine the susceptibility of the magnetic material in the microdrops, the interfacial tension $\sigma$, and the macroscopic viscosity $\eta_m$ which is roughly 100 times the solvent viscosity $\eta = 10^{-3}$ Pas. The microdrops are observed with an optical microscope and their behavior recorded through a video camera system. Alternating current is supplied in phase quadrature into two pairs of perpendicular coils to produce a uniform clockwise rotating magnetic field of intensity ranging from 50 to 1000 A/m and of frequency ranging from 4 Hz to 4 kHz.

An MF microdrop exhibits a rich and complex behavior in response to both the frequency and magnetic field strength. Complicated shapes (loops, worms, stars,...) are observed in the intermediate range of magnetic fields, while at high field, regardless of the frequency, the result is invariably a spiny starfish with a large number of arms, corotating with the field.

In zero magnetic field, the MF droplet is spherical. At any frequency the first stage of shape deformation produces an oblate ellipsoid, with its plane of symmetry having the largest cross section in the plane of the rotating magnetic field. For an axial ratio larger than 1.5, this oblate ellipsoid becomes unstable leading to the shapes of Fig. 1 which shows the behavior of a given microdrop (initial radius $R_0 = 15$ $\mu$m, susceptibility $\chi = 24$, surface tension $\sigma = 2.8 \times 10^{-6}$ J/m$^2$) as a function of field amplitude at 4 and 460 Hz. From 4 Hz to 1 kHz the final shape is

0031-9007/94/72(17)/2705(4)$06.00

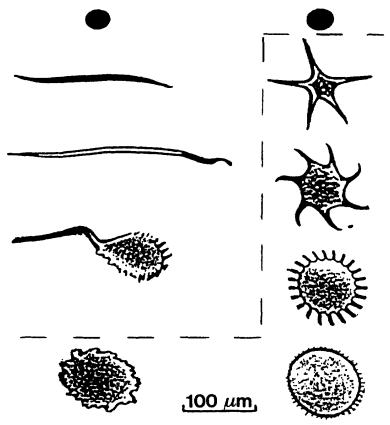


FIG. 1. Shapes of an MF drop submitted to a clockwise magnetic field rotating in the plane of observation. (Left column: $\omega/2\pi=4$ Hz; right column: $\omega/2\pi=460$ Hz). From top to bottom magnetic field strength $H_0$ is 50, 450, 630, 700, and 900 A/m. The dashed line demarcates rotating spiny starfish.

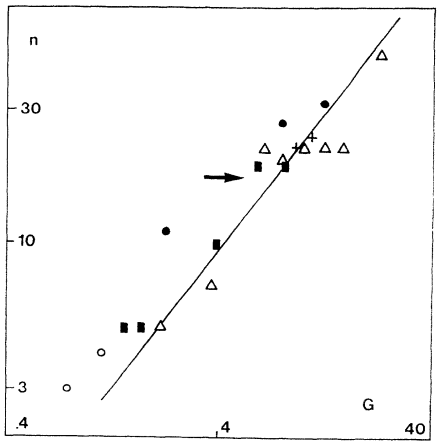


FIG. 2. Number $n$ of lateral peaks versus $G=\mu_0 H_0^2 R_D/\sigma$. The arrow points to the threshold. Slope of full line is $-1$: $n \propto H_0^2$ (+: 47 Hz; ●: 230 Hz; △: 460 Hz; ■: 1 kHz; ○: 4 kHz).

always a spiny starfish: a flat disk, crowned with peaks, that rotates clockwise as the field does. The frequency $\Omega$ of disk rotation is always very slow: The maximum value we measured is a few Hz in a rotating field of a few kHz. Observation of some dust particles inside the disk shows that this rotation is steady and close to that of solid body rotation. An important feature of the drop deformation is that, except for 4 Hz, there is no response at the frequency of excitation: The characteristic relaxation time of a drop shape perturbation is, for a sphere, $\tau_\sigma=\eta_m R/\sigma$ and here $\tau_\sigma^{-1}\simeq 2$ Hz. The drop deformation in the field plane is due to a normal stress, proportional to $\langle H_n^2\rangle$ ($H_n$ is a normal component of magnetic field) and the rotation is due to tangential stress that is proportional to $\eta\omega$ [12]. The normal stress is frequency independent and accounts for elongated and oblate shapes. The tangential stress produces the drop rotation and the evolution towards more globular conformations at high frequencies. The effect of a tangential stress due to a rotating field on an MF drop is not obvious. By analogy with current loops in diamagnetic materials [13], vortexes from individual particles cancel each other in the MF bulk, but are uncompensated at an interface, leading to a corotation of the drop. A dual phenomenon is the counter-rotation of a bubble inside a bulk of MF.

Disk diameter $R_D$ and number of arms $n$ are measured as a function of amplitude $H_0$ and frequency $\omega$ of the rotating field. In Fig. 2, the arm number of intermediate shapes and of spiny starfishes is plotted as a function of the reduced quantity $G=\mu_0 H_0^2 R_D/\sigma$ for various frequencies ranging from 4 Hz to 4 kHz. The arrow indicates the threshold (almost independent of $\omega$) at which the drop shape becomes a disk, the number of peaks being larger than 20. Whatever the frequency, the disk axial ratio $a/c$ ($a$ is the long semiaxis, $c$ the short one) is of the order of 14 at the threshold. Figure 3 is an experimental plot of $a/c$ versus magnetic bond number $\Gamma=\mu_0 H_0^2 R_0/\sigma$. For fields below the disk threshold, indicated by the arrow in Fig. 3, the lateral arms are neglected in the size determinations leading to $a/c$, as it is only the central part of the drop shape which is encountered. These determinations are insensitive to rotating field frequency; this means that, from 4 Hz to 4 kHz, stationary drop conformations can be described in a quasistatic approximation with $\omega\tau_B \ll 1$ where $\tau_B=\eta V_p/kT$ is the Brownian relaxation time of a particle of volume $V_p$ in the MF. The shape of a static MF drop is governed by a competition between its interfacial energy $E_S$ and its magnetic energy $E_M$. In a similar way as in Ref. [5], $E_S$ and $E_M$ can be written for an oblate ellipsoidal shape with magnetic field $H_c$ parallel to its large axis. Minimization of total energy with respect to $a/c$ at constant field $H_c$ and using experimental parameters $H_c^2=\langle H^2\rangle=H_0^2$, $\sigma$, and $\chi$ permits plotting the solid line of Fig. 3, which displays reasonable agreement with the data.

To understand dynamical quantities such as frequencies of drop rotation, a more general description is necessary. In this theoretical treatment, microdrops are approximated as oblate ellipsoids. We shall discuss steady shapes, rotating frequency, and conditions of instability for a general ellipsoid. Slow motions of MF in time dependent magnetic fields are ruled by the following: (a) The equation of motion

$$-\partial P/\partial x_i+\partial\sigma_{ij}/\partial x_j=0\,,$$

which relates pressure $P$ to the viscous stress tensor which is not symmetric here but includes an antisymmetric part $\sigma_{ij}^a=\frac{1}{2}\mu_0 e_{ijk}(\mathbf{M}\times\mathbf{H})_k$ ($M$ is magnetization, $H$ magnetic field, and $\mu_0$ vacuum permeability). (b) The magnetic relaxation equation [14]

$$d\mathbf{M}/dt-(\boldsymbol{\Omega}\times\mathbf{M})=\tau_B^{-1}[\mathbf{M}-\chi(\mathbf{H}-\mathbf{NM})],$$

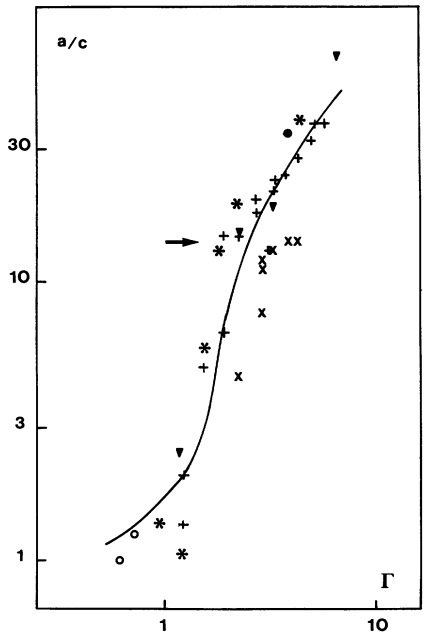


FIG. 3. Axial ratio $a/c$ of equilibrium oblate shape versus $\Gamma=\mu_0\langle H^2\rangle R_0/\sigma$. (●: 4 Hz; ×: 47 Hz; ▼: 230 Hz; +: 460 Hz; *: 1 kHz; o: 4 kHz; full theoretical line and arrow: see text).

valid close to equilibrium in the weak field limit; $\Omega$ is hydrodynamic vorticity inside the ellipsoidal drop where magnetic field is homogeneous and governed by the demagnetization tensor N.

Dynamic boundary conditions are imposed with an MF viscosity $\eta_m$ much larger than $\eta$ the viscosity of the surrounding liquid. Virial relations of the lowest order can be written as

$$U_{ik}=-\int x_k \partial P/\partial x_i dV+\int x_k \partial\sigma_{ij}/\partial x_j dV=0,$$

where $V$ is the volume of the drop. Excluding the pressure term and for $\omega\tau_\sigma>1$, the steady condition shape of the MF drop in the rotating field is given by $U_{33}-\frac{1}{2}(U_{11}+U_{22})=0$. This relationship is equivalent to that for an oblate shape given by the energy formulation leading to the solid line of Fig. 3, if $\omega\tau_B\ll 1$. Virial relations also allow us to analyze shape stability against symmetry destroying perturbations. Figure 4 is a typical plot of perturbation growth rate $\beta$ as a function of axial ratio $a/c$ of an oblate ellipsoid for different values of $\chi$. In experimental conditions ($\chi=24$) the oblate shape is unstable against a general ellipsoidal shape for $a/c\geq 1.8$ and this stability is restored for $a/c\geq 20$, which are values close to the experimental ones. Figure 4 shows that there is a critical value of $\chi$ ($\chi_c=7$) below which the oblate shape is stable for any axial ratio, over the whole range of field strengths. Angular velocity $\Omega$ of the drop is determined for $\omega\tau_B\ll 1$ from $U_{21}-U_{12}=0$ giving the following result:

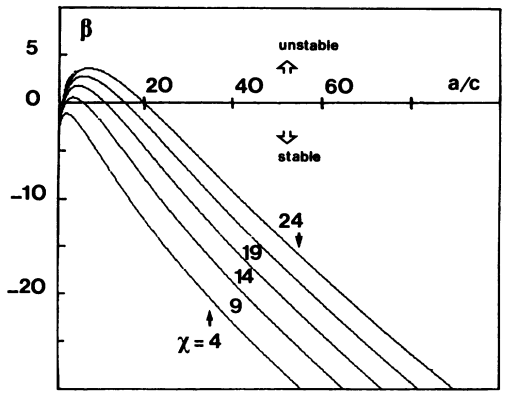


FIG. 4. $\beta$, growth rate of symmetry destroying perturbations of an oblate ellipsoid as a function of its axial ratio $a/c$ for different values of $\chi$. From bottom to top, $\chi=4$, 9, 14, 19, and 24.

$$\Omega=\frac{\mu_0\langle H^2\rangle(\omega\tau_B)^{1-\alpha}}{(1+\chi n_D)^2}\chi\frac{n_D}{2\eta}, \quad (1)$$

$n_D$ being the demagnetizing factor of the oblate droplet. The previous simple equation of magnetic relaxation was modified in obtaining this relationship to take into account the polydispersity of magnetic particles, with a standard Cole-Cole exponent $\alpha$ being introduced [15]. The field dependence of $\Omega$ is not simple: The demagnetizing factor $n_D$ is also a function of magnetic field. Figure 5 is a plot of the experimental value $\Omega_{exp}$ versus $\Omega_{calc}$ as deduced from expression (1) using experimental quantities ($\omega$, $H_0^2$, $\chi$, and $n_D$ deduced from measured axial ratio $a/c$) with $\tau_B=4\times10^{-7}$ s and $\alpha=0.65$: It leads to a mean diameter of magnetic particles of 14 nm. These orders of magnitude are consistent with usual size distributions of magnetic particles inside MF drops [11,16]. Thus internal friction and demagnetizing effects explain the large difference between field rotation frequency and rotation rate of the spiny starfish as has been observed in prior macroscopic experiments [12,17,18].

What is the basic process breeding the arms of starfish? From simple arguments it is obvious that a centrifugal force driven instability cannot account for their formation but that the standard MF peak instability mechanism should be put forward. Because the size of microdrops in Fig. 1 is steady under given operating conditions, these experiments are quite different from the experiments reported in Ref. [8]. In addition there is no contact line in our problem and the sharp tips of starfish arms are characteristic of magnetic field effects. Experimentally with MF in rotating fields, lateral peaks always crown oblate drops, their number growing roughly as $H_0^2$ (cf. Fig. 2); a simple model presented below can explain this feature.

Thus, the standard peak instability of a flat MF surface [19] submitted to a normal magnetic field is induced by thermal fluctuations of the interface which leads to local

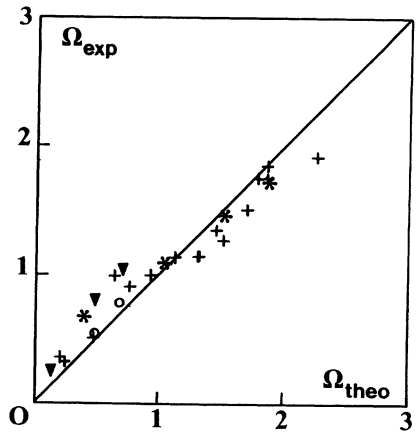


FIG. 5. Experimental frequency of drop rotation versus calculated one [expression (1)]; $\tau_B$ is taken equal to $4\times10^{-7}$ s and $\alpha=0.65$ (same symbols as in Fig. 3).

magnetic field gradients that produce destabilizing magnetic forces. Taking into account also gravity and capillarity, which stabilize the interface, the dispersion equation of the surface waves $\omega_p(k_p)$ can be written as

$$\rho\omega_p^2=\sigma k_p^2+\rho g k_p-\mu_0\chi^2 k_p^2 H^2, \quad (2)$$

where $\rho$ is MF density and $\chi\gg1$. In our case MF droplets are smaller than the capillary length, gravity is negligible, and in a rotating field $H^2=\langle H_n^2\rangle=H_0^2$. The surface is always unstable and the least stable wave vector is $k_p^*\propto\mu_0\chi^2H^2/\sigma$. The drop perimeter introduces a $k_p$ quantification leading to a number of arms $n^*=R_Dk_p^*$ proportional to $H_0^2$, as observed experimentally; see Fig. 2 with but a discrepancy of order $\chi^2$ in the coefficient. In fact, a more rigorous calculation can be performed looking at the deformation of the free surface of an infinite MF cylinder, submitted to a high-frequency rotating field $H_0$, oriented transversely to the axis. In that case, the dispersion equation for circumferential waves is [20]

$$\rho\omega_n^2=n\left[\frac{\sigma(n^2-1)}{R_D^3}-2\mu_0\frac{(\mu-1)^3}{(\mu+1)^3}\frac{H_0^2(n-1)}{R_D^3}\right]. \quad (3)$$

The highest rate of growth corresponds to

$$n^*=\tfrac{4}{3}\mu_0\frac{(\mu-1)^3}{(\mu+1)^3}H_0^2\frac{R_D}{\sigma}$$

in agreement with experimental results of Fig. 2, providing only a small discrepancy of the order of 2 in the prefactor.

In summary, we have explored the rich behavior of an MF drop submitted to a rotating magnetic field. Because of the asymmetry of the MF stress tensor, unexpected shapes are observed. Regardless of the field frequency, the final state is always a spiny starfish corotating with the field. A model was proposed accounting for the oblate shape stability in large fields and for the large difference between the rotating frequency of magnetic field and that of the MF drop. A magnetic peak instability leads to the formation of arms of rotating starfish. However, some points remain as open questions. These include understanding the drop behavior before the onset of spiny starfish as well as aspects of the middle shapes such as slowly rotating distorted worms and reptating snakes that strongly depend on frequency of the magnetic field.

We are greatly indebted to Dr. V. Cabuil for providing us with ferrofluid, to J. Servais for the time dependent magnetic field setup, and to R. Goldstein, A. Levelut, R. Rosensweig, and D. Salin for helpful discussions. Laboratoire d'Acoustique et Optique de la Matière Condensée is associated with the Centre National de la Recherche Scientifique.

*Also at Université Paris 7, Tour 23, 2 place Jussieu, 75251 Paris Cedex 05, France.

[1] H. Poincaré, *Figures d'Équilibre d'Une Masse Fluide* (Ed. J. Gabay, Paris, 1990), reedition of 1902 lecture.
[2] S. Chandrasekhar, Proc. R. Soc. London A **286**, 1 (1965).
[3] G. Taylor, Proc. R. Soc. London A **280**, 383 (1964).
[4] G. Taylor, Proc. R. Soc. London A **146**, 501 (1934).
[5] J.-C. Bacri and D. Salin, J. Phys. (Paris), Lett. **43**, L649 (1982).
[6] L. H. Tanner, La Recherche **17**, 184 (1986).
[7] P. G. de Gennes, Rev. Mod. Phys. **57**, 827 (1985).
[8] F. Melo, J.-F. Joanny, and S. Fauve, Phys. Rev. Lett. **63**, 1958 (1989).
[9] J. B. Brzoska, F. Brochard-Wyart, and F. Rondelez, C.R. Acad. Sci. Paris II **312**, 819 (1991).
[10] S. M. Troian, E. Herbolzheimer, S. A. Safran, and J. F. Joanny, Europhys. Lett. **10**, 25 (1989).
[11] J.-C. Bacri, R. Perzynski, D. Salin, V. Cabuil, and R. Massart, J. Colloid. Interface Sci. **132**, 43 (1989).
[12] R. E. Rosensweig, J. Popplewell, and R. J. Johnston, J. Magn. Magn. Mater. **85**, 171 (1990).
[13] R. P. Feynman, *The Feynman Lectures on Physics* (Addison-Wesley, Reading, MA, 1970), Vol. II.
[14] M. I. Shliomis, Zh. Eksp. Teor. Fiz. **61**, 2411 (1971) [Sov. Phys. JETP **34**, 1291 (1971)].
[15] E. J. Blums, A. O. Cebers, and M. M. Mayorov, *Magnetic Fluids* (Riga, Zinatne, 1989).
[16] J.-C. Bacri, R. Perzynski, D. Salin, V. Cabuil, and R. Massart, J. Magn. Magn. Mater. **62**, 36 (1986).
[17] R. Mailfert and A. Martinet, J. Phys. (Paris) **34**, 197 (1973).
[18] A. V. Lebedev and A. F. Pshenichnikov, Magn. Gidrod. **1**, 7 (1991).
[19] R. E. Rosensweig, *Ferrohydrodynamics* (Cambridge Univ. Press, Cambridge, 1985).
[20] A. O. Cebers and S. Lacis, in Proceedings of 1st SAASMF, Goiania, Brasil, October 1993 (to be published).